Chapter

Determination on Fluidization Velocity Types of the Continuous Refined Salt Fluidized Bed Drying

Bui Trung Thanh and Le Anh Duc

Abstract

After the centrifugation stage, refined salt particles have rather high moisture content; therefore, the moist salt particles in contact with each other will stick together in a short time. In particular, the moist salt particles will stick together faster and tighter and form a larger unit when they are exposed to drying hot air. For this reason, the refined salt was dried by rotary drum dryers with vibrating balls distributed along the drum or a vibrating fluidized bed dryers. These drying methods make poor product sensory quality, low product recovery efficiency, while also lead to an increase of heat and electricity energy consumption. In order to increase the efficiency of refined salt drying technology by conventional continuous fluidized bed dryers, the chapter focuses on the study of aerodynamic properties of refined salt grains in the continuous fluidized particle layer. The content of the chapter presents theoretical and empirical methods to determine fluidization velocity types in designing a continuous fluidized bed dryer.

Keywords: refined salt, solid particles, aerodynamic, minimum fluidization velocity, homogeneous fluidization, bed fraction, fluidized bed dryer

1. Introduction

1.1 Preface

The phenomenon in which solid particles float in a gas stream and have a liquid-like property is called a fluidized bed. This phenomenon of fluidization in gas or liquid flow was discovered by Fritz Winkler in the 1920s [1]. This one was investigated by Lewis et al. and had been raised to fluidized theory [2]. The first commercial fluidized bed dryer was installed in USA in 1948 [3]. The fluidized bed technology is used for drying of bulk materials, includes examples such as: vibrating fluidized bed dryer, normal fluidized bed dryer without vibrating device and pulsed fluidized bed dryer.

Mathematical modeling and computer simulation of grain drying are now widely used and become an important tool for designing new dryers, for analyzing existing drying systems and for identifying drying conditions [4]. Identifying the drying conditions is necessary to establish the optimal protocol for ensuring seed quality [5]. To solve the simulation models, equations concerning aerodynamic properties such as the gas stream velocity and particle velocity are the most important components. The aerodynamic properties are affected by shape, density and size of particles [6].

Order	Function of gases	Function of solid materials	Equipment in practice
1	Heat carrier	Materials do not react to gases	• Heaters supply to materials • Heat exchangers with heat recovery
2	Loading and transportation of particle materials	Materials do not react to gases	Pneumatic solid particle carrier
3	Heat carrier and material loading and transportation	Materials do not react to gases	Aerodynamic dryers
4	Chemical agents	• Chemical reaction • Activated material for chemical reactions • As inert material which is used in fluidized bed combustion of boiler	• The burner burns • Gasification equipment • Catalytic reconstitution • Oxidation equipment • Processing of metallurgical surfaces and annealing furnace
5	Agitation	Materials do not react to gases	Mixer of different materials in the tank

Table 1.
Relations and functions of gas interacting with solid particle in real production.

In recent years, the fluidized bed technology has been concerned in the application in the sugar drying and refined salt drying in Vietnam. In the scope of this chapter, we discuss the issues related to the hydrodynamics of refined salt particles in the gas stream at ambient temperature and temperature equivalent to that of drying particle. The focus of this chapter is to determine the velocity values of the gas through the particle layer to form the minimum, homogeneous and critical fluidized layers.

In industrial manufacturing practice, we often encounter the contact, interaction between solid-particle materials and gases. These interaction phenomena are described in **Table 1**.

1.2 Applied materials in fluidized bed drying technology

According to Abrahamsen and Geldart [7], the two most important factors affecting the fluidization characteristic of the particle layer are particle size and particle density.

Geldart [8] visually observed the various conditions and classified fluidizable particles into four groups: A, B, C and D. As a result, the classification was related to the influence of the average particle size and particle density on the properties of the fluidized layer, as depicted in **Figure 1** and **Table 2**.

According to the content of this chapter, we focus on approaching, researching and experimenting on the mechanism and principle of interaction between air and the applied material in fluidized bed drying. The approach method is to arrange a stream of heat-carrying air blowing from the bottom of the particle chamber through a gas distributor (the holes arranged at an angle to the cross section of the tank). Hot air stream is evenly distributed and touches the surface of particles in tank (the particle layer was on the gas distributor). The continuous air stream ensures that the contact of particle surfaces with the gas flow is consecutive. The nature of the gas flowing through the particle layer may be laminar, turbulent, or transition flow at the material contact surface. The inflow of hot air affects the velocity of the interaction between the gas stream and the material.

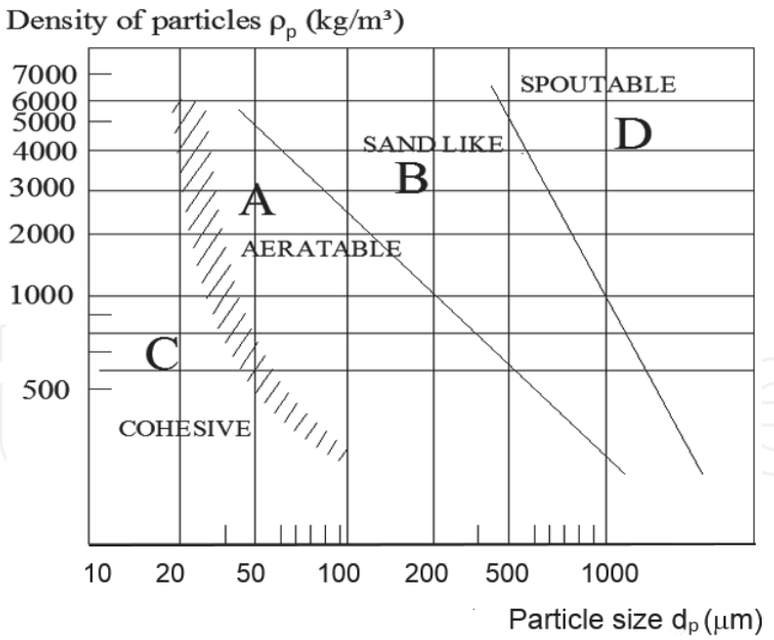

Figure 1.
Diagram of the Geldart classification of particles [9, 10].

1.3 Basic concept of fluidized particle layer and principle of fluidized particle layer creation

When the material layer is fluidized, its state is converted from a fixed bed to a dynamic state. The particle layer has liquid-like properties. The surface area of the particles contacting with the fluid increases, and therefore the heat transfer ability from fluid to particles rapidly rises.

In order for the fluidization phenomena to occur in the bulk material layer, the air stream must have sufficient pressure and velocity. The air stream flows upward, passes through the particle materials (follow the linear increment) through uncountable air holes of the distributor, which are arranged at the bottom of the particle material layer. When the velocity of air stream is small, pressure exerted on particles is small, the particle layer maintains its original fixed bed (the state from 0 before point A, **Figure 2**). As the air velocity is increased further, the aerodynamic traction appears, which has opposite effect of the gravitational force of the particles, causing the expansion of particle layers in a volume, and the particles begin to move apart from each other (at point A, **Figure 1**).

By further raising the velocity of air stream to the critical value, the friction force between the particles and air is equal to the weight of particles. At this time, the vertical component of the compression pressure is eliminated, the upward-pulling force equals the downward gravity, causing the particle material to be suspended in the air stream. When the gas velocity reaches the critical value, the particle material layer will be converted to complete fluidization state, called the fluidization particle layer and having the liquid-like properties (position from A to B in **Figure 2**).

By further increasing the velocity of the gas, the bulk density of the particle layers continues to decrease, its fluidization becomes more violent, until the particles no longer form a bed and are swept up and fallen down in the fluidization motion (position from B to C, **Figure 2**). At this time, each particle material is covered with gas flow, the intensity of the heat and material transfer occurs violently. When granular material is fully fluidized, the bed will conform to the volume of the chamber, its surface remaining perpendicular to gravity; objects with a lower

Particle group characteristics	C group	A group	B group	D group
Particle size (μm)	0–3	$30 \leq d_p \leq 100$	$100 \leq d_p \leq 1000$	≥ 1000
Density (kg/m^3)	Smallest	1400	400–4500	Lower than other materials
The most obvious characteristics of group	• Particles are cohesive and linked • Difficult fluidization	• Easy fluidization • Dense phase expands stably before bubbling starts	• Starting on bubble creation at the minimum fluidized velocity value	• The rough solid particles
Typical granulars	• Flour • Cement	• Milk flour • FCC granular	• Construction sands	• Pebbles in rice • Coffee beans, wheat, lead shot
Properties of fluidization layer				
Particle layer expansion	• Channeling possibilities in the particles layer easily	• The large bed expansion before bubbling is started • The minimum fluidization velocity is smaller than minimum bubbling	Medium	Difficult to fluidize evenly (low)
Properties of air bubbles	• Do not form bubble	• It does not form bubble fluidization • There is a maximum bubble size	• The bubbles rise faster than the interstitial gas • Bubbles are large and grow rapidly and coalescence, as they rise through the bed	• Bubbles rise more slowly than the rest of the gas percolating through the emulsion
Property of mixed solid particles	Very low	High	Solids' recirculation rates are smaller	Low
Spaying	None	None	Only occurs in the upper layer	• It occurs • Only occur in under layers

Table 2.
The classification of fluidization properties of particle groups according to Geldart [9, 11].

density than the bed density will float on its surface, bobbing up and down, while objects with a higher density sink to the bottom of the bed.

Fluidization has many applications in many technologies of manufacturing practice, such as mixing different types of granular materials; fluidized bed drying; cooling grain after drying; supporting interaction between chemicals in the fluidized bed; granulation technology; film coating technology of medicine and pharmacy; manufacturing technology through the combined use of organic and inorganic fertilizers; and biomass fuel combustion technology in fluidized bed.

To clarify the dynamics of the fluidized beds for application in refined salt drying in the fluidized bed, the theoretical and experimental issues determining the velocity of gas through the particle layers to form different fluidized layers are described as follows.

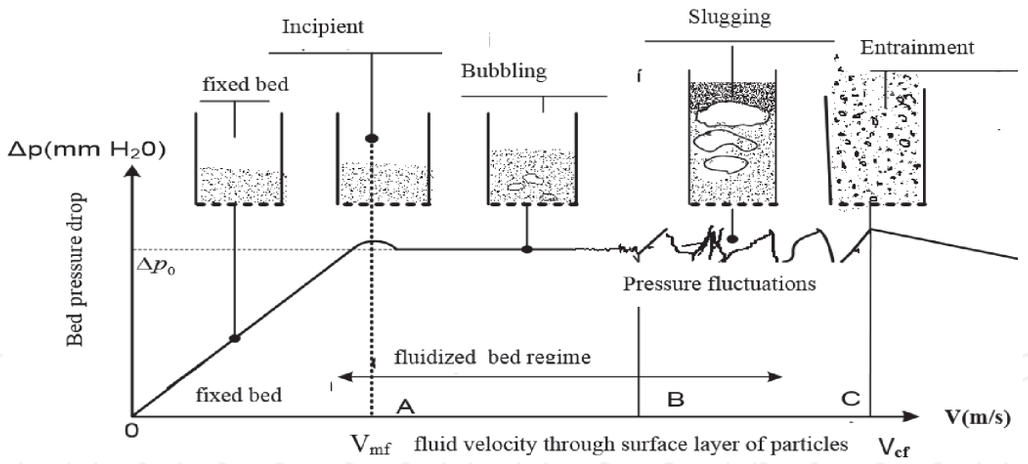

Figure 2.
Particle layer states with gas velocity changing [10].

2. Methodology

2.1 Determination of the minimum fluidization velocity from publications

2.1.1 Determination of V_{mf} using the Ergun equation

When the air stream having sufficient pressure and velocity passes through the static spherical particle layers, they begin to expand (the particles become "flexible"). In this condition, it is called the minimum particulate fluidization state and is described by the modified equation of Ergun (see position A in **Figure 1**) [12].

$$\frac{\Delta P}{H_{mf}} = \frac{150\mu_f(1-\varepsilon_{mf})^2 V_{mf}}{\varepsilon_{mf}{}^3 d_p^2} + \frac{1.75(1-\varepsilon_{mf})\rho_f V_{mf}{}^2}{\varepsilon_{mf}{}^3 d_p} \tag{1}$$

For particles of arbitrary shapes, the pressure drop of air stream at the minimum fluidization state is represented by Eq. (2). The spherical value of particle material got in the Eq. (1) [10] is given by:

$$\frac{\Delta p}{H_{mf}} = 150\frac{(1-\varepsilon_{mf})^2}{\varepsilon_{mf}{}^3}\frac{\mu_f V_{mf}}{(\phi d_m)^2} + 1.75\frac{(1-\varepsilon_{mf})}{\varepsilon_{mf}{}^3}\frac{\rho_f V_{mf}{}^2}{\phi d_m} \tag{2}$$

For the particle layer to be converted from a fixed state to a fluidization state, the pressure of air stream must be large enough to overcome the weight of the particle layers and it is determined by Eq. (3) [10].

$$\Delta p = \frac{m}{\rho_p A}\left(\rho_p - \rho_f\right)g \tag{3}$$

In Eq. (3), it is considered that there was no interaction force between particles in layer and no interaction between particles and the wall of the tank. So, that did not cause the pressure increasing effect. Thus, the pressure drop of the air stream was constant while increasing the gas velocity from the smallest fluidization velocity to the value when the entrainment process of particles occurred (position C, **Figure 2**).

In Eqs. (1) and (2), it is also shown that the pressure drop of the gas stream that is generated through the fluidized particle layer is depended on the particle size (d_p), the bed voidage (ε) and the gas temperature ($t^\circ C$). According to Eq. (3), the

pressure drop of the gas stream through the particle layers is dependent upon the material mass (m), the gas distributor grate area (A), particle density (ρ_p) and gas density (ρ_f). Thus, we could calculate the minimum fluidization velocity value (V_{mf}), which was based on Eqs. (1)–(3) for non-spherical particles by solving Eq. (4).

$$\frac{m.H_{mf}}{\rho_p.A}\left(\rho_p-\rho_f\right)g = 150\frac{\left(1-\varepsilon_{mf}\right)}{\varepsilon_{mf}{}^3}\frac{\mu_f V_{mf}}{\left(\phi d_p\right)^2}+1.75\frac{\rho_f V_{mf}{}^2}{\varepsilon_{mf}^3}\frac{}{\phi d_p} \tag{4}$$

The minimum fluidization velocity (V_{mf}) is the root of Eq. (4), which is based on available parameters, such as the height of minimum fluidization bed (H_{mf}), the mass of particles in the air distributor (m), the area for gas distribution or called cross-sectional area of the bed (A), particle density (ρ_p), air density (ρ_f), mean particle diameter (d_p), spherical degree of particles (ϕ) and void fraction at minimum fluidization particle layer (ε_{mf}).

Commonly, the sphere degree of particles (ϕ) must be determined in experiments [10]. The spherical degree of refined salt particles was found out by Bui [13–15]. Theoretically, in order to fluidize the particle layer, the actual weight of the solid particles must be equal to the force exerted on the particle layers and that is equal to the pressure drop across the bed (ΔP) multiplied by the cross-sectional area of the chamber (A). A minimum fluidization layer which must have determined layer thickness (H_{mf}), void fraction (ε_{mf}), then the expanded volume of the fluidized particles (U) has the value of the Eq. (5):

$$U = (1-\varepsilon_{mf}).A.H_{mf} \tag{5}$$

And the actual gravity of the particle mass has a value of:

$$W = (1-\varepsilon_{mf})\left(\rho_p-\rho_f\right).A.H_{mf}.g \tag{6}$$

The balance of the real gravity components of the particle mass and the upward force exerted on the particle mass of the gas flow was calculated according to

$$\Delta P = (1-\varepsilon_{mf})\left(\rho_p-\rho_f\right).H.g \tag{7}$$

Substituting Eq. (8) into Eq. (1) or Eq. (2) yields Eq. (9).

$$\left(1-\varepsilon_{mf}\right)\left(\rho_p-\rho_f\right).H_{mf}.g = 150\frac{\left(1-\varepsilon_{mf}\right)^2}{\varepsilon_{mf}{}^3}\frac{\mu_f V_{mf}}{\left(\phi d_p\right)^2}+1.75\frac{\left(1-\varepsilon_{mf}\right)}{\varepsilon_{mf}{}^3}\frac{\rho_f V_{mf}{}^2}{\phi d_p} \tag{8}$$

$$150\frac{\left(1-\varepsilon_{mf}\right)}{\phi^2\varepsilon_{mf}^3}\,\mathrm{Re}_{mf}+\frac{1.75}{\phi\,\varepsilon_{mf}^3}\,\mathrm{Re}_{mf}^2 = Ar \tag{9}$$

Giving physical parameters of particle and gas into the Eq. (8), velocity (V_{mf}) was found out. In case of very small particles, the gas stream regime through the particle layer was laminar flow and the minimum fluidization velocity should be calculated by the Ergun equation [12]. In case of $Re_{mf} < 1$, we use Eq. (9) to calculate the minimum fluidization velocity of gas.

2.1.2 Determination of V_{mf} by the correlation of Re_{mf} and Archimeter (Ar)

When gas passes through the particle bulk, which can have any shape, the minimum fluidization Reynolds coefficient (Re_{mf}) is determined by Eq. (10).

$$\mathrm{Re}_{mf} = \frac{\rho_{mf}.V_{mf}.d_p.\phi}{\mu_f} \tag{10}$$

Eq. (11) describes the correlation between Ar and Re_{mf} with void fraction at minimum fluidization particle layer (V_{mf})

$$Ar = 150\,\frac{(1-\varepsilon_{mf})}{\phi^2\,\varepsilon_{mf}^3}\,\mathrm{Re}_{mf} + \frac{1.75}{\phi\varepsilon_{mf}^3}\,\mathrm{Re}_{mf}^2 \tag{11}$$

Archimeter (Ar) is determined by Eq. (12) for particles of any shape.

$$Ar = \frac{\rho_f\left(\rho_p - \rho_f\right)g\left(\phi d_p\right)^3}{\mu_f^2} \tag{12}$$

Set up Eq. (13):

$$\frac{\rho_f\left(\rho_p - \rho_f\right)g\left(\phi d_p\right)^3}{\mu_f^2} = 150\,\frac{(1-\varepsilon_{mf})}{\phi^2\,\varepsilon_{mf}^3}\,\mathrm{Re}_{mf} + \frac{1.75}{\phi\,\varepsilon_{mf}^3}\,\mathrm{Re}_{mf}^2 \tag{13}$$

Substituting physical parameters into the Eq. (12), which includes the particle density (ρ_p), the gas density at the temperature of minimum fluidization velocity (ρ_f), the air dynamic viscosity (μ_f), spherical degree of particle (ϕ), void fraction at the minimum fluidization velocity (ε_{mf}), mean particle diameter (d_m) [13–15] and getting Ar number value into the Eq. (13). Then, we solved the quadratic equation to find out the root of equation Re_{mf} in Eq. (10), we got only the positive value. Thus, we calculated the minimum fluidization velocity (V_{mf}) from Eq. (10).

2.1.3 Determination of V_{mf} by the Kozeny-Carman correlation

Kozeny-Carman gave the formula of calculation of the minimum fluidization velocity for a very small particle size with the $Re_{mf} < 10$ in Eq. (14) described in Yates [16].

$$V_{mf} = \frac{g\left(\rho_p - \rho_f\right)}{150\mu_f}\,\frac{{\varepsilon_{mf}}^3}{1-\varepsilon_{mf}}\,\phi^2 d_p^2 \tag{14}$$

For spherical particles or sphericity equivalent, the bed voidage of the minimum fluidization $\varepsilon_{mf} = 0.4 \div 0.45$.

2.1.4 Determination of V_{mf} by correlation of Wen and Yu

In case of the unavailability of the sphericity of particles, we determine the minimum fluidization velocity (V_{mf}) by using of the experimental correlation of Wen and Yu [17]. An empirical formula of calculation of the void fraction at minimum fluidization particle layers in Eq. (15) or Eq. (16) with the available sphericity degree of particle (ϕ) or the calculation of the sphericity degree of particle (ϕ) in case void fraction (ε_{mf}) at minimum fluidization particle layer is available, which was also described by Wen and Yu equation (cited in Howard, 1989) [10].

$$\frac{1-\varepsilon_{mf}}{\phi^2 \varepsilon_{mf}^3} \approx 11 \text{ or } \frac{1}{\phi \varepsilon_{mf}^3} \approx 14 \tag{15}$$

We can use the calculation of the void fraction at minimum fluidization particle layers from the other correlation, which is also converted from Wen and Yu.

$$\varepsilon_{mf} = \left(\frac{0.071}{\phi}\right)^{1/3} \tag{16}$$

It is based on the calculation of the void fraction (ε_{mf}) (at position A in **Figure 2**) of Eq. (15) or Eq. (16) and substituting the obtained ε_{mf} value into the Ergun Eq. (2), we have Eq. (17).

$$Ar = 1650\ \mathrm{Re}_{pmf} + 24.5\ \mathrm{Re}_{pmf}^2 \tag{17}$$

Using the calculated Ar number from Eq. (12) and substituting the Ar value into Eq. (17), we obtain Eq. (18) to calculate the particle Reynolds number at the minimum fluidization velocity (Re_{mf}).

$$\mathrm{Re}_{mf} = \frac{-1650 \pm \{1650 + (4 \times 24.5\ Ar)\}^{1/2}}{2 \times 24.5} \tag{18}$$

Taking the positive square root, we get Eq. (19):

$$\mathrm{Re}_{mf} = \left(33.7^2 + 0.0408\ Ar\right)^{1/2} - 33.7 \tag{19}$$

It was applied to calculate for solid particles with size larger than 100 μm [10]. From the Re_{mf} value that was found out in the Eq. (19), V_{mf} is calculated according to Eq. (10). In case of solid particles with small size (C group of Geldart, 1973) in the specified temperature conditions, the V_{mf} value is calculated in Eq. (20) by Wen and Yu.

$$V_{mf} = 7.90.10^{-3} d_p^{1.82} \left(\rho_p - \rho_f\right) 0.94 \mu_f^{-0.83} \tag{20}$$

2.1.5 Determination of V_{mf} by the correlation of Beayens and Geldart

For solid spherical particles with diameters ranging from 0.05 to 4 mm (0.05 mm < d_p < 4 mm) and particle density ranging from 850 to 8810 kg/m^3 (850 kg/m^3 < ρ_p < 8810 kg/m^3), the method of calculation of V_{mf} was proposed by Beayens and Geldart as shown in Eq. (21) [18].

$$Ar = 1823\ \mathrm{Re}_{mf}^{1.07} + 21.7\ \mathrm{Re}_{mf}^2 \tag{21}$$

Then the V_{mf} can be calculated from Eq. (22) in case of available solid particle and gas parameters.

$$V_{mf} = \frac{9.125 \times 10^{-4} \left(\left(\rho_p - \rho_f\right) g\right)^{0.934} d_p^{1.8}}{\mu_f^{0.87} \rho_p^{0.66}} \tag{22}$$

2.1.6 Determination of V_{mf} by correlation of Goroshko

The minimum fluidization velocity of spherical particles was determined by correlation shown in Eq. (23) by Goroshko described in Howard [10, 19].

$$a\ \mathrm{Re}_{mf}^{2} + b\ \mathrm{Re}_{mf} - Ar = 0 \tag{23}$$

where

$$a = \frac{1.75}{\phi\,\varepsilon_{mf}^{3}} \text{ and } b = \frac{150\left(1-\varepsilon_{mf}\right)}{\phi^{2}\,\varepsilon_{mf}^{3}} \tag{24}$$

We get ϕ is 1.0 (ϕ = 1) then solving the Eq. (23) take the spherical degree value, we have the Eq. (25).

$$\mathrm{Re}_{mf} = \frac{-b + \left(b^{2} + 4aAr\right)^{1/2}}{2a} \tag{25}$$

Multiplying $\left(b + \sqrt{b^{2} + 4aAr}\right)$ by the numerator and denominator of Eq. (25), we have the Eq. (26)

$$\mathrm{Re}_{mf} = Ar\left\{\frac{b}{2} + \left[\left(\frac{b}{2}\right)^{2} + aAr\right]^{1/2}\right\}^{-1} \tag{26}$$

And its value was determined by Eq. (27) by Goroshko:

$$\mathrm{Re}_{pmf} = \frac{Ar}{b + \sqrt{aAr}} \tag{27}$$

Eq. (27) is different from Eq. (26) by the added value $\left(\frac{b}{2}\right)^{2} + aAr = \frac{b}{2} + \sqrt{a.Ar}$. There is a difference in $\mathrm{Re_{mf}}$ value between the Goroshko equation and Ergun equation. The $\mathrm{Re_{pmf}}$ of Goroshko equation [Eq. (27)] is smaller than $\mathrm{Re_{mf}}$ of Ergun [Eq. (26)]. This deviation interval depends on the value of Archimeter (Ar). Thus, we have a correlation equation, which is described in Eq. (28).

$$\frac{\mathrm{Re}_{mf}\,(Ergun)}{\mathrm{Re}_{pmf}\,(Goroshko)} = \frac{b + \sqrt{aAr}}{\left\{b/2 + \left[(b/2)^{2} + aAr\right]^{1/2}\right\}} \tag{28}$$

2.1.7 Determination of V_{mf} following Goroshko and Todes equation

The minimum fluidization velocity ($\mathrm{V_{mf}}$) of sphericity particles was defined from the $\mathrm{Re_{mf}}$ by Goroshko et al. in Eq. (29) [19].

$$\mathrm{Re}_{pmf} = \frac{Ar}{150\frac{1-\varepsilon_{mf}}{\varepsilon_{mf}{}^{3}} + \sqrt{\frac{1.75}{\varepsilon_{mf}^{3}}Ar}} \tag{29}$$

In case of non-spherical particles with different sizes, the $\mathrm{Re_{pmf}}$ value was error from 15–20% in case we use the Eq. (29) of calculation described in [20]. In the case of rapid calculation, we considered the bed voidage of the minimum fluidization state to be equal to the bed voidage at static particle layers ($\varepsilon_o = \varepsilon_{mf} = 0.4$), and the $\mathrm{Re_{mf}}$ is calculated in Eq. (30) [21].

$$\mathrm{Re}_{mf} = \frac{Ar}{1400 + 5.22\sqrt{Ar}} \tag{30}$$

2.1.8 Determination of V_{mf} following Leva

From the formula of Carman-Kozan $k = \frac{g.\rho_f.\varepsilon_{mf}}{\mu_f k_c S}$ described in (as cited in Leva, [22]) yield the formula to define the minimum fluidization velocity [22, 23].

$$V_{mf} = \frac{5 \times 10^{-3}(\phi d_p)^2\left(\rho_p - \rho_p\right)g{\varepsilon_{mf}}^3}{\mu_{mf}(1-\varepsilon_{mf})} \tag{31}$$

The Leva formula is used in case of Reynolds to be smaller than 10 ($Re_{mf} < 10$). In case of Reynolds to be larger than 10 ($Re_{mf} > 10$), there is an adjustment factor added into this formula.

2.1.9 Determination of V_{mf} according to Kunii-Levenspiel

The formula of Kunii-Levenspiel was simplified from the Ergun formula and it gave out two cases of calculation of the minimum fluidization velocity. In the first case for solid particles of small size with $Re_{mf} < 20$, we have to use Eq. (32).

$$V_{mf} = \frac{(\phi d_p)^2}{150\mu_f}\frac{\left(\rho_p - \rho_f\right)g{\varepsilon_{mf}}^3}{(1-\varepsilon_{mf})} \tag{32}$$

We have to use Eq. (33) for the larger particle size with Reynolds number larger than 1000 ($Re_{mf} > 1000$).

$${V_{mf}}^2 = \frac{(\phi d_p)\left(\rho_p - \rho_f\right)g.{\varepsilon_{mf}}^3}{1.75\rho_f} \tag{33}$$

2.1.10 Determination of V_{mf} based on the bed voidage problem

There is a correlation equation of particle mass balance at the minimum fluidization state (fluidization without bubbles), which was created by Kunii and Levenspiel as shown in Eq. (34).

$$g.H_0(1-\varepsilon_0)\rho_p.A = (1-\varepsilon_{mf})\rho_p g.H_{mf} \tag{34}$$

Thus, we can obtain a correlation as shown in Eq. (35).

$$\frac{H_{mf}}{H_0} = \frac{(1-\varepsilon_0)}{1-\varepsilon_{mf}} \tag{35}$$

According to Ginzburg, described in [18], the bed voidage of minimum fluidization and height of particle layer are calculated by Eq. (36) and Eq. (37).

$$\varepsilon_{mf} = \varepsilon_0 \times 10\% \tag{36}$$

$$H_{mf} = H_0 \times 10\% \tag{37}$$

McCabe et al. proposed $\varepsilon_{mf} = 0.4 \div 0.45$ for the spherical particle [24]. The bed voidage of minimum fluidization particle layers was 0.5 ($\varepsilon_{mf} = 0.5$) for larger particle size. The bed voidage is equal to 1.0 ($\varepsilon_t = 1.0$) when the particle layers are attracted to the gas stream (see position C in **Figure 2**).

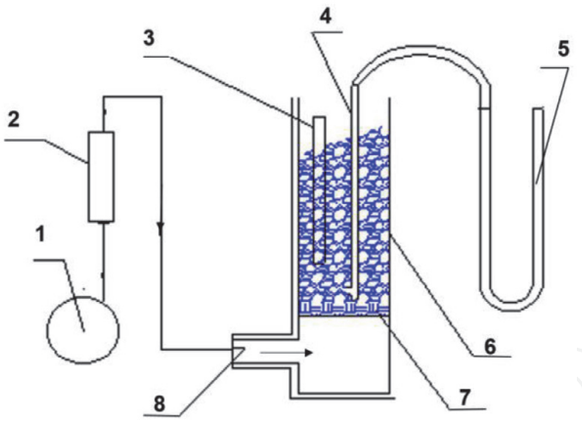

Figure 3.
Model for determination of the minimum fluidization velocity. 1. Centrifugal fan; 2. air heater; 3. thermometer for surface particle temperature measurement; 4. pitot tube for measurement of dynamic pressure and total pressure of air; 5. U-manometer; 6. chamber of fluidization; 7. air distributor; 8. drying air inlet.

2.2 Physical model of experiment

Experimental arrangement of determining the minimum fluidization velocity is shown in **Figure 3**.

In order to gradually increase the bed surface velocity of hot air via the particle layers, the air fan (1) is equipped with an inverter to change the rotation of the fan motor.

2.3 Experimental equipment

The instruments in experiments include a moisture analyzer (Axis AGS100, Germany), measurement error ± 0.01%; a digital electronic scale (Satorius MA45, Germany), measurement error ± 0.001 g; an air velocity meter (Extech SDL350 Taiwan), measurement error ± 0.01 m/s and a digital thermometer (WIKA CTH6300, Germany), measurement accuracy 0.001°C. This instrument has two measuring rate modes including fast at 4/s and slow at 1/s; an inclined manometer (T10, UK), measured range is 0–280 mmwg with error ± 0.1% and a pitot pipe (PT6300, 304 Germany), measurement range is 0–400 mmwg with error ± 0.1%. For measurement on the bulk density and density of refined salt particles, we used instruments such as Graduated pipet, buret, graduated cylinder, all of them made in Germany with error measurement ± 0.01 ml. The HCl acid is used for density measurement of refined salt particles.

No.	Equipment/parts	Technical parameter
1	Drying air fan	Flow: 0.63 m^3/s; total pressure: 1244 Pa; motor power: 2.2 kW
2	Electrical heater	Overall dimension (L × W × H): 600 × 630 × 275 mm; heating power: 1.0 kW; number of heater bars: 6
3	Drying chamber	Overall dimension (L × W × H): 1750 × 300 × 350 mm Fabrication material: SUS304
4	Salt dust settling chamber	Overall dimension (L × W × H): 1750 × 450 × 350 mm Fabrication material: SUS304

Table 3.
The basic parameters of the continuous fluidized bed dryer for experiment by authors.

2.4 The materials of refined salt particles

The material of refined salt particles was supplied by a combined hydraulic separating-washing-grinding machine in the saturated saltwater condition and which was dried by a continuous centrifugal machines. Samples of refined salt were randomly taken at different sizes at Vinh Hao salt company in Binh Thuan Province, Bac Lieu salt company and Sea salt Research Center of Vietnam for analysis (**Table 3**) [14].

3. Results and discussions

The above section presented nine methods to calculate minimum fluidization velocity based on the physical parameters of particles and physical thermal parameters of gas stream. These parameters were obtained from experiments in combination with the correlation calculation or empirical formulas.

In order to have the basis of comparison and accuracy evaluation of each calculating method in comparison with the empirical method, the theoretical calculation was carried out for refined salt particles with diameters of 1.5 mm, 1.2 mm, 0.9 mm, 0.6 mm and 0.3 mm. On the other hand, to achieve empirical result, samples of dried refined salt particles (of which mean-diameter was determined) were taken randomly from a combined hydraulic-separating-washing-crushing machine, presenting various particle sizes of the raw material that was put in the dryer.

3.1 Results of theoretical and empirical calculations for determining V_{mf} of refined salt particles

3.1.1 Some primary conditions for determining the V_{mf} by theoretical calculations

When calculating the pressure drop across a refined salt particle layer, we relied on the empirical results of physical parameters of particles and air (summarized in **Table 4**). Specific notes for each calculating method are as follows:

a. Calculation based on Ergun equations and correlations of pressure

   Applying to calculate the minimum fluidization velocity (V_{mf}) for refined salt particles with the fixed bed height (H_0) is 30 mm, the bed voidage (ε_0) is 0.5 using Eqs. (35) and (36) to find out the minimum fluidization state including $H_{mf} = 1.1 \times H_0 = 33$ mm; bed voidage $\varepsilon_{mf} = 1.1 \times \varepsilon_0 = 0.56$. Using the spherical degree value of refined salt particle is 0.71 ($\phi = 0.71$) and other parameters were taken from the **Table 5** which described in Bui (2009). Then we use the Ergun equations to calculate the minimum fluidization velocity. It is recommended that Re_{mf} had no limit [13–15].

b. Calculation based on the correlation between (Re_{mf}), (Ar) and Kozeny-Carman

   In these two calculation methods, the parameters in the calculations are taken from the empirical results according to **Table 5**.

c. Determination of the (V_{mf}) value according to Wen and Yu

   According to Wen and Yu methods, the bed voidage of the refined salt particle layer at minimum fluidization state (ε_{mf}) was unknown, but we had

Determination of the minimum fluidization velocity according to theoretical and empirical methods											
No	**d_h (mm)**	**Minimum fluidization velocity**									
		Ergun	**Re andAr**	**Ko and Ca**	**Wen and Yu**	**Gedar**	**Go**	**Todes**	**Leva**	**Kunii and Levenspiel**	**Empirical methods**
1	1.65	1.327	0.939	3.149	0.5414	0.45	1.1223	1.122	2.362	3.149	0.8
2	1.35	1.094	0.736	2.108	0.4002	0.331	0.9022	0.902	1.581	2.108	0.6
3	1.05	0.826	0.518	1.275	0.2625	0.219	0.6653	0.665	0.956	1.275	0.58
7	**0.953**	**0.731**	**0.445**	**1.05**	**0.2209**	**0.186**	**0.586**	**0.586**	**0.788**	**1.05**	**0.55**
4	0.75	0.522	0.298	0.651	0.1416	0.123	0.4188	0.419	0.488	0.651	0.42
5	0.45	0.22	0.115	0.234	0.0524	0.05	0.1863	0.186	0.176	0.234	0.2
6	0.225	0.058	0.029	0.059	0.0132	0.014	0.0537	0.054	0.044	0.059	0.15

*The bold values in **Table 4** refers to the common average particle size for commercial refined salt in the Vietnamese market.*

Table 4.
Theoretical calculation results of minimum fluidization velocity for refined salt particles from equations and empirical correlation formulas of published authors, which compare to the experimental results of the physical model of author.

Technical parameter	Symbol	Unit	Value	Ref.
Refined salt particle diameter	d_p	mm	1.65; 1.35; 1.05; 0.75; 0.45; 0.225	[13, 14] [15]
Average diameter of particle	d_m	mm	0.953	
Static bed voidage	ε_0		0.51	
Bed voidage in minimum fluidization velocity	ε_{mf}		0.56	
Particle density	ρ_p	kg/m^3	2138	
Bulk density	ρ_b	kg/m^3	982	
Spherical degree of particle	ϕ		0.71	
Gas density (at 160°C)	ρ_f	kg/m^3	0.815	
Dynamic viscosity (at 160°C)	μ_f	kg/m.s	2.45×10^{-5}	
Fixed refined salt particle bed height	H_0	m	30	

Note: The particle diameter d = 0.953 is the average diameter of the salt particles.

Table 5.
Physical parameters of refined salt grains and physical air.

the value of spherical degree particle from experiments (see **Table 5**). We put the value of spherical degree into Eq. (5) or Eq. (16) and found out the value of bed voidage (ε_{mf}) from which the velocity value of gas passing through the minimum fluidization particle layer (V_{mf}) was calculated.

d. Determination of V_{mf} according to Groshko-Todes

In this method, we also used the results of physical parameters of refined salt particles and air supplied to the dryer from **Table 5** to calculate Ar number. The Re_{mf} is determined by using Eq. 2 and the obtained result was multiplied by the error coefficient k = 1.2 and it was considered as the result of calculation of Re_{mf} for non-spherical salt particles (described by Lebedev, [21]). In addition, in Todes method there was another calculation by using Eq.(29) based on the available results of the minimum fluidization velocity (ε_{mf} = 0.4). We put this value into Eq. (15) and we found out the spherical degree of salt particles according to correlation given by Wen and Yu. Then we put this value into Eq. (12) to determine Ar number. By replacing Eq. (29) with the value of Ar number, we found out $Re_{mf,}$ from which we could calculate V_{mf} value by using Eq. (10).

e. Determination of V_{mf} by the formula of Beayens-Geldart, Goroshko, Leva, and Kunii-Levenspiel

The minimum fluidization bed velocity (V_{mf}) was determined by using theoretical calculation of formulas of Beayens-Geldart, Goroshko, Leva, and Kunii-Levenspiel with the available physical parameters of refined salt particles and gas given in **Table 5** [18, 19, 22, 25, 26]. **Table 4** shows the calculated results from the formulas of authors published last time.

3.1.2 Primary conditions for determining V_{mf} by experimental method

A model in **Figure 3** and the other of fluidized bed dryer in **Figure 4** was designed by authors to define the minimum fluidization velocity of refined salt

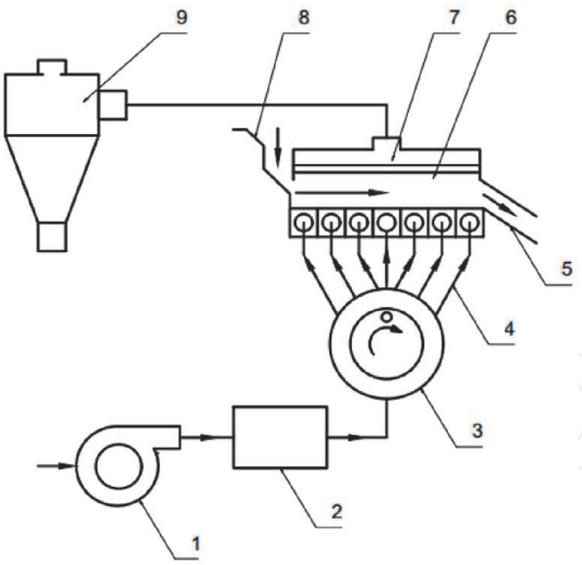

Figure 4.
The model of continuous fluidized bed dryer used in experiments. 1. Air fan; 2. heating chamber; 3. air supplier; 4. air duct; 5. product outlet; 6. drying chamber; 7. dust separation chamber; 8. inlet feeder; 9. cyclone dust collector.

particles in experiment. The dryer model was designed with its capacity of 48 kg/hour, the height of salt particle layer at the static bed was 30 mm ($H_0 \geq 30$ mm). In the experiments, the authors determined the minimum fluidization velocity (V_{mf}) for refined salt particles with diameter 1.65, 1.35, 1.05, 0.9, 0.65, 0.4 and 0.3 mm. The experimental results of determination of the minimum fluidization velocity of the particle layers with the different particle sizes are shown in **Table 4**. Besides, these experimental minimum fluidization velocity values were also compared with results of theoretical models that were published by authors presented in the methodology part above (**Figure 5**).

3.2 Discussions

- The obtained values of minimum fluidization velocity (V_{mf}) calculated by the Ergun equation and the correlation between Re_{mf} number and Ar number for

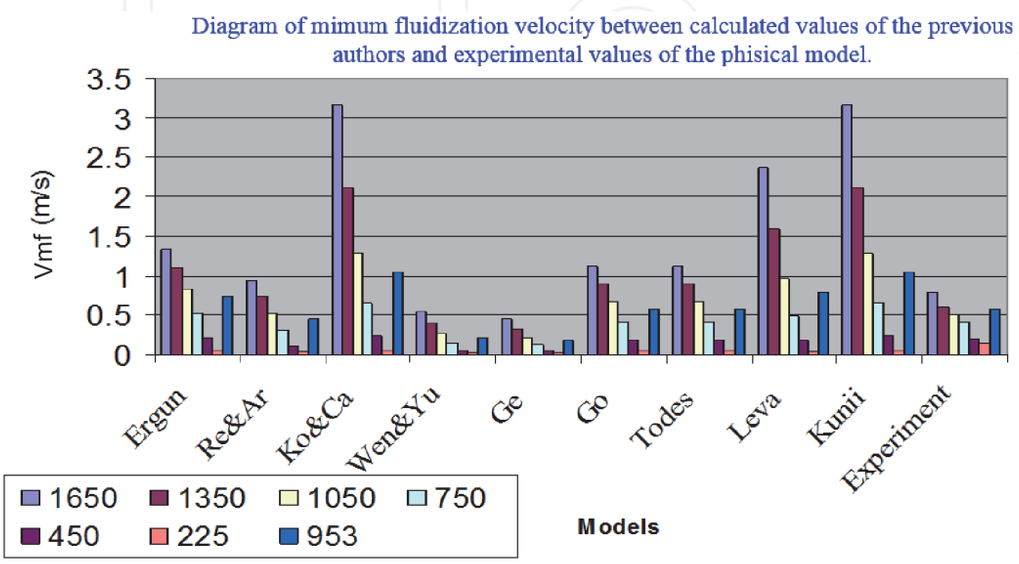

Figure 5.
Comparison of the minimum fluidization air velocity between calculated values of published authors and experimental values of the model [14].

all particle sizes agreed well with the experimental values. The value of Re_{mf} number varies from 0.3 to 51.7. Particles with sizes d_p = 0.225; 0.45 and 0.75 had the tendency for laminar flow.

- The obtained values of minimum fluidization velocity (v_{mf}) determined by the Kozeny-Carman and Kunii equations for particles with diameter greater than 1 mm ($d_p > 1$ mm) were much larger than experimental values ($V_{tmf} > > V_{emf}$). While, with particles having diameter smaller than 1 mm ($d_p < 1$ mm), the result of calculation was nearly equal to the experimental values. Notably, the void fraction value of the minimum fluidization state from 0.4 to 0.5 (ε_{mf} = 0.4–0.5) the calculation result matches the experimental value.

- By using the correlation of Wen and Yu to calculate void fraction at (ε_{mf}) knowing the spherical properties of particle, we obtained values that were much smaller than the experimental value. The Re_{mf} number varied from 0.07 to 21.1.

- When using the correlation between Re_{mf} and Ar, the obtained values of minimum fluidization velocity fit quite well to experimental results. Reynolds values vary from 0.16 to 36.6.

- The minimum fluidization velocity that was calculated according the correlation between Re_{mf} and Ar number of Beayens and Geldart (Eq. (19)) gave reasonable results.

- The obtained values by using the Goroshko and Todes formula in Eq. (28) were nearly equal to the experimental values.

- The calculated value of V_{mf} according to Beayens and Geldart was the lowest in comparison to other methods.

- The difference between the values of Re_{mf} calculated according to Goroshko and Ergun was lower than 10–20% for particles that lie in the range of Re_{mf} number from 0.28 to 43.7 (Re_{mf} = 0.28–43.7). The obtained values of velocity value (V_{mf}) for particles with diameter smaller than 0.9 mm ($d_p < 0.9$ mm) were closer to the experimental value in comparison with particles with diameter larger than 0.9 mm ($d_p > 0.9$ mm).

- The minimum fluidization velocity that was calculated by Leva formula was only suitable for particles with diameter smaller than 0.75 mm ($d_p < 0.75$ mm) and value of Re_{mf} number smaller than 10 ($Re_{mf} < 10$). The regime of air flow through the particle layer is laminar flow.

- The calculation method of the minimum fluidization velocity according to the Kunii and Levenspiel equations was suitable for particle with diameter d_p = (0.225; 0.45; 0.75 mm) and the results were appropriate under the conditions $Re_{mf} < 20$, and the calculation result was close to the experimental value.

3.3 Determination of air velocity through the particle layer at the optimum fluidization regime (V_{of})

The optimal fluidization velocity V_{of} was in the region from A to C (**Figure 2**). It meets the conditions:

$$V_{mf} < V_{hf} < V_{cf} \tag{38}$$

The air superficial velocity value from A to C (**Figure 2**) was determined by the two standard equations as follows:

The air velocity through the solid particle layer at the optimum fluidization regime (V_{of}) was calculated according to Fedorov standard (Fe) by Eq. (39) (as cited in Lebedev [21]), with refined salt particles and drying air parameters taken from **Table 5** (t_f = 160°C) [13, 15].

$$Fe = \phi d_p \left(\frac{4g\left(\rho_p - \rho_f\right)\rho_f}{3\mu_f^2}\right)^{1/3}$$
$$= 0.71 \times 0.956 \times 10^{-3}.\left(\frac{4 \times 9.8(2138 - 0.815)0.815}{3.\left(2.45 \times 10^{-5}\right)^2}\right)^{1/3} = 32 \tag{39}$$

According to Ginzburg (1973), Re_{hf2} was calculated by Eq. (40) [20, 27].

$$\mathrm{Re}_{hf2} = (0.19 \div 0.285)\ \mathrm{Fe}^{1.56} -> \mathrm{Re}_{hf2} = 0.237 \times 32^{1.56} = 53 \tag{40}$$

The homogeneous fluidization velocity (V_{hf1}) was calculated by Eq. (41).

$$V_{hf2} = \frac{\mu_f.\mathrm{Re}_{hf}}{\rho_f.d_p} = \frac{2.45 \times 10^{-5} \times 53}{0.815 \times 0.956 \times 10^{-3}} = 1.6 m/s \tag{41}$$

Reynolds value at homogeneous fluidization velocity (V_{hf1}) was measured according to Archimedes standard by Eq. (42) [20].

$$\mathrm{Re}_{hf1} = (0.22 \div 0.33) \times \mathrm{Ar}^{0.52} \tag{42}$$

where Ar was calculated by Eq. (12):

$$Ar = \frac{\rho_f\left(\rho_p - \rho_f\right)g\left(\phi d_p\right)^3}{\mu_f^2}$$

Substituting parameters of air and refined salt particles into the Eq. (12),

$$Ar = \frac{9.81 \times \left(0.71\left(956 \times 10^{-6}\right)\right)^3 \times 0.815 \times (2138 - 0.815)}{\left(2.45 \times 10^{-5}\right)^2} = 8818.4$$

The Ar value is 8818.4

Therefore, Re_{hf1} = 0.275 × $(8818.4)^{0.52}$ = 66.917 = 31.53.

The homogeneous fluidization velocity (V_{hf1}) was calculated by Eq. (43).

$$V_{hf1} = \frac{\mu_f.\mathrm{Re}_{hf}}{\rho_f \phi d_p} = \frac{2.45 \times 10^{-5} \times 31.53}{0.815 \times 0.956 \times 10^{-3}} = 0.99\ \mathrm{m/s} \tag{43}$$

Re-calculating the homogeneous fluidization velocity (V_{hf1}) by using the experimental equation Eq. (44) [27].

From **Table 4** for the specific case: V_{mf} = 0.55 m/s and particle diameter was 0.953 mm.

$$V_{hf1} = (2 \div 3) \times V_{mf} = (2 \div 3) \times 0.56 = (1.12 \div 1.68)\ \text{m/s} \tag{44}$$

Both V_{hf1} and V_{hf2} met the conditions of the Eq. (38). Selecting the optimum velocity V_{of}:

$$V_{of} = (V_{hf1} + V_{hf2})/2 = (0.99 + 1.66)/2 = 1.33\ \text{m/s}$$

Re-calculating the standard Reynolds number at reasonable fluidization state (Re_{of}) under the condition of optimum fluidization velocity (V_{of} = 1.33 m/s)

$$V_{of} = \frac{\mu_f . \mathrm{Re}_{of}}{\rho_f . d_p} \tag{45}$$

or

$$\mathrm{Re}_{of} = \frac{\phi d_p \rho_f V_{of}}{\mu_f} = \frac{0.71\left(0.956 \times 10^{-3}\right) 0.815 \times 1.33}{2.45 \times 10^{-5}} = 30$$

The value of optimum Reynolds number (Re_{of}) was 30 (Re_{of} = 30).

The void fraction of the particle layer at the reasonable fluidization state was determined by the Zabrodski formula (Eq. 46) (described in Lebedev, [21]).

$$\varepsilon_{hf1} = \left(\frac{18\,\mathrm{Re}_{ohf} + 0.36\,\mathrm{Re}_{ohf}^2}{Ar}\right)^{0.21} = \left(\frac{18 \times 30 + 0.36(30)^2}{8818.4}\right)^{0.21} = 0.61 \tag{46}$$

Re_{hf2} could be recalculated according to the correlation between Re_{hf2} and Ar Eq. (47).

$$\mathrm{Re}_{hf2} = (0.22 \div 0.33)\mathrm{Ar}^{0.52} = 0.275 \times (8818.4)^{0.52} = 31 \tag{47}$$

Substituting value of Re_{hf2} into Eq. (46), we re-calculated the homogeneous fluidization void fraction (ε_{hf}) by Eq. (48).

$$\varepsilon_{hf2} = \left(\frac{18\,\mathrm{Re}_{hf} + 0.36\,\mathrm{Re}_{hf}^2}{Ar}\right)^{0.21} = \left(\frac{18 \times 31 + 0.36(31)^2}{8818.4}\right)^{0.21} = 0.62 \tag{48}$$

These two calculation methods generated almost identical results.

3.4 Calculation of the critical air velocity flowing through the fluidization particle layer

In order to have a basis for determining the reasonable dimension of separating chamber of fluidized bed dryer (the chamber was located above the fluidization particle drying tank) and to limit removal of materials from the drying chamber, we defined the theoretical critical velocity (also called the final velocity).

From the calculation result of Re_{mf} of the minimum fluidization state (Re_{mf} = 10.032), this parameter of the air stream through the particle layer in the transition flow was in range $1 < Re_{mf} < 500$.

According to the equation of Haider and Levenspiel (described in Wen-ChingYang) [28, 29], the critical velocity was calculated by Eq. (49).

$$V_{cf} = \left[\frac{4\left(\rho_p - \rho_f\right)g}{3\rho_f C_D}\phi d_p\right]^{1/2} = \left[\frac{4(2138 - 0.815)9.81}{3 \times 0.815 \times C_D}0.71 \times 0.953\right]^{1/2} \quad (49)$$

With resistance coefficient (C_D) (described in Wen-ChingYang) [27, 28] given by

$$C_D = \frac{18}{\mathrm{Re}^{3/5}} = \frac{18}{(10.032)^{3/5}} = 4.5 \quad (50)$$

So, the critical velocity at position C (**Figure 2**) in the specific case had the value:

$$\begin{aligned} V_{cf} &= \left[\frac{4\left(\rho_p - \rho_f\right)g}{3\rho_f C_D}\phi d_p\right]^{1/2} \\ &= \left[\frac{4(2138 - 0.815) \times 9.81}{3 \times 0.815 \times 4.5}\left(0.71 \times 956 \times 10^{-6}\right)\right]^{1/2} = 2.3m/s \end{aligned} \quad (51)$$

In fact, during the drying process, to ensure the drying productivity and quality, the dryer operator must observe the fluidization particle layer and adjust the inlet doors of drying air capacity at appropriate the air velocity value in the range from A to C (**Figure 2**) and the correlation of velocity types $V_{mf} < V_{hf} < V_{cf}$.

We re-calculated the void fraction of particle layer with average particle diameter $d_p = \phi d_m$ = 0.953 mm at the theoretical critical velocity in fluidization particle layer condition.

$$\mathrm{Re} - \text{calculating } \mathrm{Re}_{cf}: \mathrm{Re}_{cf} = \frac{\phi d_p.\rho_f.V_{of}}{\mu_f} \quad (52)$$

Substituting the above value into Eq. (52), we get:

$$\mathrm{Re}_{cf} = \frac{0.71 \times \left(956 \times 10^{-6}\right) \times 0.815 \times 2.3}{2.4 \times 10^{-5}} = 0.53.$$

Using Eq. (46) to re-calculate the void fraction of particle layer at the complete fluidization state:

$$\varepsilon_{tf} = \left(\frac{18\,\mathrm{Re}_{cf} + 0.36\,\mathrm{Re}_{cf}^2}{Ar}\right)^{0.21} = \left(\frac{18 \times 53 + 0.36 \times (53)^2}{8818.4}\right)^{0.21} = 0.73$$

When the void fraction of particle layer was 1 (ε = 1), the fluidization particle layer turned to the transport regime in the air stream (called pneumatic transportation).

4. Conclusions

Most of the used correlations in the calculations and the formulas given by the authors, as mentioned above, were derived from the experiments with temperature close to the ambient temperature. So, when we use them in calculations in specific cases, they should consider the accuracy. The extrapolation should be used in the cases of the states at the temperature higher than the ambient temperature.

The mentioned theoretical calculations show the necessity for the determining of the minimum fluidization velocity of the solid particle layer with high accuracy. The sphericity of particle and void fraction of the particle layer were often not known, therefore it is required to get their values from the range of experimental variables. Empirically, the void fraction of the particles in the minimum fluidization layer at the ambient temperature is not the same as that in the increasing gas temperature.

The best method to determine the minimum fluidization velocity is to conduct the experiments. Firstly, we directly measured the pressure drop across the particle layer when the air velocity gradually decreased. Secondly, we built the graphs and read the results of the minimum fluidization velocity value.

However, if we were forced to find out the fluidization velocity without carrying out experiments to measure the pressure drop across the particle layer, the best way would be to determine the void fraction at the minimum fluidization velocity. Then we calculated the spherical property of the particle using the Ergun equations or correlation between Ar and Re_{mf} in Eqs. (10)–(12) to count out the minimum air velocity through the particle fluidization layer. This velocity value also had accuracy close to the experimental one.

The average particle diameter considered spherical degree of the particles of different sizes was 953 μm (d_m = 953 μm). This diameter represented the size of the particles in dry grinding technology with the hammer crusher. It is also in the common size distribution range of the combined washing-grinding hydraulic-separation technology in Vietnam's market. Besides, the particle diameter of 953 μm (d_p = 953 μm) is also used in calculating the value of all types of velocity, characterized for the medium particle size of the refined salt production technology in Vietnam.

We calculated the values of three characteristic velocity types of fluidized bed drying for particles with average size $d_m = d_p$ = 953 μm, including the minimum fluidization velocity V_{mf} = 0.55 m/s with void fraction ε_{mf} = 0.56; reasonable fluidization velocity V_{hf} = 1.33 m/s corresponding to the void fraction of particle layer ε_{hf} = 0.615; and the critical velocity of the air flow through the particle bulk V_{cf} = 2.3 m/s with the void fraction value of fluidization particle layer ε_{cf} = 0.73.

In fact, during the drying process, to ensure the drying productivity and quality, the dryer operator must observe the fluidization particle layer and adjust the inlet doors of drying air capacity at appropriate air velocity value in the range from A to C (**Figure 2**) to make sure the correlation of velocity types $V_{mf} < V_{hf} < V_{cf}$.

Nomenclature

A	cross sectional area of the bed
m^2	area for gas distribution
H	height of the bed, m
Ar	Archimedes number, dimensionless
H_0	initial bed height, m

ε_0	void fraction at static particle layer
H_{mf}	minimum fluidization bed height, m
ε_{mf}	void fraction at minimum fluidization particle layer
ΔP	pressure drop across the bed, N/m^2
ε_{hf}	void fraction at homogeneous fluidization particle layer
Re	Reynolds number
ε_{tf}	terminal void fraction
Re_{mf}	Reynolds number at the minimum fluidization velocity
Re_{hf}	Reynolds number at the homogeneous fluidization velocity
d_p	spherical particle diameter, m
ϕd_m	equivalent spherical mean diameters, m
Re_{cf}	Reynolds number at the fluidization terminal velocity
ϕ	sphericity degree, dimensionless
Re_{of}	Reynolds number at the optimum fluidization velocity
Fe	Fedorov standard, dimensionless
V	bed surface velocity or superficial velocity, m/s
g	acceleration due to gravity, m/s^2
V_{mf}	minimum fluidization velocity, m/s
ρ_p	solid particle density, kg/m^3
V_{tmf}	theoretical minimum fluidization velocity, m/s
ρ_b	particle bulk density, kg/m^3
V_{emf}	experimental minimum fluidization velocity, m/s
ρ_f	air density, kg/m^3
V_{hf}	homogeneous fluidization velocity, m/s
Kcc	Kozeny-Carman coefficient
V_{ohf}	optimum homogeneous fluidization velocity, m/s
m_p	mass of particles, kg
V_{cf}	terminal velocity or critical velocity, m/s
m_b	mass of particles bulk, kg
μ	air dynamic viscosity, kg/ms
S_s	specific surface area, cm^{-1}, cm^2/g
U	cubic volume of particle layer, m^3
W	weight of particle, mass, N

Author details

Bui Trung Thanh[1*] and Le Anh Duc[2*]

1 Industrial University of Ho Chi Minh City, Vietnam

2 Nong Lam University, Ho Chi Minh City, Vietnam

*Address all correspondence to:
buitrungthanh@iuh.edu.vn and leanhduc@hcmuaf.edu.vn

References

[1] Tavoulareas S. Fluidized-bed combustion technology. Annual Reviews. 1991;**16**:25-27

[2] Lewis WK, Gilliland ER, Bauer WC. Characteristics of fluidized particles. Industrial and Engineering Chemistry. 1949;**41**:1104-1117. DOI: 10.1021/ie50497a059

[3] Zahed AH, Zhu JX, Grace JR. Modelling and simulation of batch and continuous fluidized bed dryers. Drying Technology. 1995;**13**:1-28. DOI: 10.1080/07373939508916940

[4] Han JW, Keum DH, Kim W, Duc LA, Cho SH, Kim H. Circulating concurrentflow drying simulation of rapeseed. Journal of Biosystems Engineering. 2010;**35**(6):401-407. DOI: 10.5307/JBE.2010.35.6.401

[5] Hong SJ, Duc LA, Han JW, Kim H, Kim YH, Keum DH. Physical properties of rapeseed (II). Journal of Biosystems Engineering. 2008;**33**(3):173-178. DOI: 10.5307/JBE.2008.33.3.173

[6] Duc LA, Han JW. The effects of drying conditions on the germination properties of rapeseed. Journal of Biosystems Engineering. 2009;**34**(1):30-36. DOI: 10.5307/JBE.2009.34.1.030

[7] Abrahamsen AR, Gedart D. Behaviour of gas-fluidized beds of fine powders part I. Homogeneous expansion. Powder Technology. 1980;**26**:47-55. DOI: 10.1016/0032-5910(80)85006-6

[8] Geldart D. The effect of particle size and size distribution on the behaviour of gas-fluidized beds. Powder Technology. 1972;**6**:201-215

[9] Geldart D. Types of gas fluidization. Powder Technology. 1973;**7**:285-292. DOI: 10.1016/0032-5910(73)80037-3

[10] Howard JR. Fluidized Bed Technology: Principles and Application. Publisher Taylor and Francis Group; 1989. p. 214

[11] Rhodes M. Fluidization of particles by fluids. In: Educational Resources for Particles Technology. Melbourne, Australia: Monash University; 2001. pp. 1-39

[12] Ergun S. Fluid flow through packed columns. Chemical Engineering Progress. 1952;**48**:9-94

[13] Bui TT. Determination on geometrical parameters of refined salt particle applying of fluidized particle lay drying. Journal of Heat Science and Technology. 2009;**86**:10-13

[14] Bui TT. Determination on hydrodynamic parameters in fine salt drying in a model of fluidized bed dryer. Journal of Heat Science and Technology. 2009;**90**:13-17

[15] Bui TT. Researching and determining on basic physical parameters of refined salt particles to apply in the calculation and designing of continuous fluidized bed. Journal of Vietnam Mechanical Engineering. 2009;**146**:8-31 and 48

[16] Yates JG. Fundamentals of Fluidized-Bed Chemical Processes. 1st ed. Oxford: Butterworth-Heinemann; 1983. p. 236

[17] Wen CY, Yu YH. A generalized method for predicting the minimum fluidized velocity. AICHE Journal. 1966;**12**:610-612

[18] Baeyens J, Geldart D. Predictive calculations of flow parameters in gas fluidized bed and fluidization behavior of various powders. In: Proceedings of

the International Symposiu on Fluidization and its Applications; 1973

[19] Goroshko VD, Rozenbaum RB, Todes OM. Approximate laws of fluidized bed hydraulics and restrained fall. Izvestiya Vysshikh Uchebnykh Zavedenii, Neft i Gaz. 1958;**1**:125-131

[20] Tran VP. Calculation and Designing on the Drying System. Hanoi: Education Publishing House; 2002

[21] Lebedev PD. Calculation and Design of Drying Equipmet. Moscow, Leningrad: Gosenergoizdat; 1963. p. 320 (in Russian)

[22] Leva M. Fluidization. New York: McGraw-Hill; 1959. p. 281

[23] Carman PC. Fluid flow through granular beds. Transactions, Institution of Chemical Engineers. 1937;**15**:150-166

[24] McCabe WE, Smith JC, Harriott P. Unit Operations of Chemical Engineering. 6th ed. New York: McGraw Hill; 2001. p. 1132

[25] Kunii D, Levenspiel O. Various kinds of contacting of a batch of solids by fluid. In: Fluidized Engineering. Huntington, NY: Robert E. Krieger Publishing Co.; 1977. pp. 24-56

[26] Kunii D, Levenspiel O. Fluidization engineering. 2nd ed. Boston: Butterworth-Heinemann; 1991. p. 49

[27] Ginzburg AS. Theoretical and Technical Basis of Drying Food Products. Moscow: Pishchevaya Promyshlennost; 1973. p. 528 (in Russian)

[28] Yang WC. Particle characterization and dynamics. In: Yang WC, editor. Handbook of Fluidization and Fluid-Particle System. New York: Marcel Dekker; 2003. pp. 1-29

[29] Yang WC. Flow through fixed beds. In: Yang W-C, editor. Handbook of Fluidization and Fluid-Particle System. New York: Marcel Dekker; 2003. pp. 29-53